

# High-brightness water-window electron-impact liquid-jet microfocus source

P. Skoglund,<sup>a)</sup> U. Lundström, U. Vogt, and H. M. Hertz

*Department of Applied Physics, Biomedical and X-Ray Physics, Royal Institute of Technology, SE-10691 Stockholm, Sweden*

(Received 11 November 2009; accepted 19 January 2010; published online 24 February 2010)

We demonstrate stable high-brightness operation of an electron-impact water-jet-anode soft x-ray source. A 30 kV, 7.8 W electron beam is focused onto a 20  $\mu\text{m}$  diameter jet resulting in water-window oxygen line emission at 525 eV/2.36 nm with a brightness of  $3.0 \times 10^9$  ph/(s  $\times \mu\text{m}^2 \times \text{sr} \times \text{line}$ ). Monte Carlo-based modeling shows good quantitative agreement with the experiments. The source has potential to increase the x-ray power and brightness by another 1–2 orders of magnitude and fluid-dynamical jet instabilities is determined to be the most important limiting factor. The source properties make it an attractive alternative for table-top x-ray microscopy. © 2010 American Institute of Physics. [doi:10.1063/1.3310281]

Soft x-ray instrumentation such as, e.g., water-window (2.3–4.4 nm, 539–282 eV) x-ray microscopes,<sup>1</sup> typically rely on high-brightness synchrotron radiation sources. Clearly the scientific impact would be higher if laboratory systems could be operated with short exposure times. However, this requires a laboratory source which in addition to a bending-magnetlike brightness and photon flux also demonstrates high stability and user-friendly reliable long-term operation. In the present paper we demonstrate such a laboratory source with stable and scalable line-emission at  $\sim 525$  eV.

Presently, only laser-plasma and discharge sources have sufficient brightness, power, and stability to allow operational laboratory water-window applications.<sup>2–4</sup> Coherent sources<sup>2</sup> such as high-harmonics and x-ray lasers lack either power, stability, or line width. For integration with applications requiring long-term and stable operation the regenerative target of the liquid-jet laser plasma<sup>3,5</sup> has proven valuable and it enabled the first high-resolution water-window laboratory x-ray microscopy.<sup>6</sup> Although this source provides the necessary brightness and stability, the long-term high-average-power operation requires complicated and expensive laser technology, making it less attractive to many potential users of laboratory water-window microscopy.

In contrast, conventional electron-impact microfocus sources are simple, stable, and reliable but do not provide sufficient brightness and power in the soft-x-ray region. Recent progress on liquid-metal-jet anodes have paved the way for increasing the hard x-ray brightness and power of microfocus sources 2–3 orders of magnitude by use of the liquid-metal-jet-anode concept.<sup>7,8</sup> Furthermore, stable hard x-ray emission from nonmetal-jets (methanol) was recently demonstrated.<sup>9</sup> However, all high-brightness work on this class of sources has so far been performed in the hard x-ray regime. Early soft x-ray experiments on water jets were limited by jet instabilities at 0.6 W on a 10  $\mu\text{m}$  diameter jet.<sup>10</sup>

In the present paper we demonstrate stable high-brightness oxygen  $K_{\alpha}$  line emission in the soft x-ray water-window range from a 30 kV electron-impact water-jet source. This 525 eV/2.36 nm line-emission is suitably positioned for x-ray microscopy in the lower part of the water-window. The source is stably and reliably operated at 7.8 W

e-beam power onto a 20  $\mu\text{m}$  diameter water jet. This is more than an order of magnitude higher power than previous soft x-ray experiments.<sup>10</sup> Furthermore, we investigate the limitations of the source and conclude that it has significant potential for increasing the power and brightness by another 1–2 orders of magnitude, thereby attaining the brightness of the laser-plasma sources.

The electron/water-jet interaction and the x-ray emission are modeled with the general-purpose Monte Carlo simulation package PENELOPE.<sup>11</sup> This code is applicable from a few 100 eV to approximately 1 GeV and uses databases with reliable cross sections and interaction data for the elements. The typical uncertainty in the 0.5 kV emission range is 20%.<sup>11</sup> In our simulations the code has been adapted to a cylindrical target geometry. For target material we use water (H and O), cooled by evaporation to 273 K and density 1.00 g/cm<sup>3</sup>.

The key system parameters, the 30 kV electron-beam energy and the 20  $\mu\text{m}$  diameter jet, were determined from simulations. The goal was a 10–20  $\mu\text{m}$  diam x-ray spot (suitable for x-ray microscopy<sup>3</sup>) and a high conversion efficiency. Nearly 100% of the energy of 30 kV electrons is absorbed in a 17–18  $\mu\text{m}$  path length. This makes 30 kV favorable to higher energies despite the fact that higher energies are easier to focus. For example, only 30% of a 50 kV beam is absorbed in 20  $\mu\text{m}$  water. The 30 kV electrons provide a  $<15$   $\mu\text{m}$  full width at half maximum (FWHM) absorption spot. Lower energies provide a too small longitudinal x-ray spot. The short path length also allows the use of a small-diameter water jet, e.g., 20  $\mu\text{m}$ , which is favorable from a vacuum perspective.

Figure 1(a) shows the experimental arrangement. The major components are the electron gun with its magnetic electron focusing lens, the water jet, and the x-ray detector equipment. These components are operated inside a turbo-pumped vacuum system. The custom-built 30 kV e-gun is based on a 100  $\mu\text{m}$  LaB<sub>6</sub>-cathode. It delivers an electron beam which is focused by the magnetic lens to an estimated 10  $\mu\text{m}$  diameter spot on the water jet. The insert (Fig. 1(b)) depicts the interaction region. The water jet is produced by forcing the liquid through a  $\sim 20$ - $\mu\text{m}$ -orifice tapered glass nozzle. The driving force is formed by 20 and 50 bars of nitrogen pressure, resulting in jet speeds of approximately 40

<sup>a)</sup>Electronic mail: peter.skoglund@biox.kth.se.

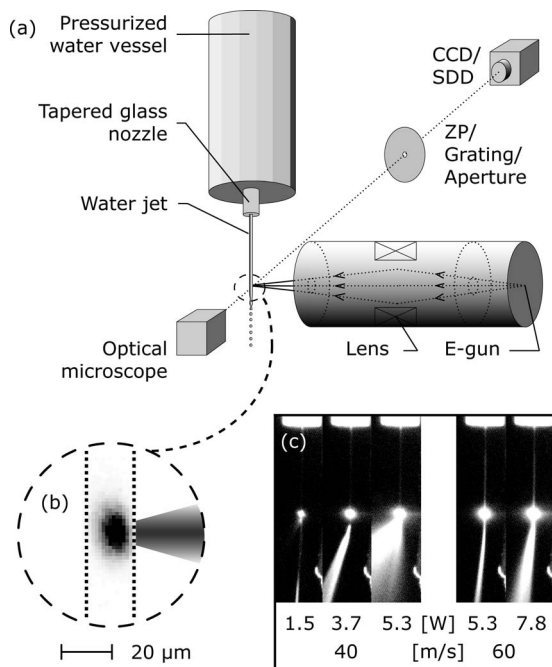


FIG. 1. Experimental arrangement (a). The inserts depicts e-beam/water-jet interaction area and the resulting x-ray spot (b) and optical imaging of the jet at different e-beam powers (1.5–7.8 W) and jet velocities (40 and 60 m/s) (c).

and 60 m/s, respectively. The remaining water is collected in a liquid-nitrogen-cooled dump. The interaction between the water jet and the electron beam results in  $\sim 525$  eV  $K_{\alpha}$  x-ray oxygen line emission and broad-band bremsstrahlung.

The interaction between the e-beam and the water jet results in significant evaporation making it necessary to carefully design the vacuum system to ensure long-term operation of the  $\text{LaB}_6$  cathode. We use a two-stage differentially pumped system. The 1 mbar nozzle chamber is separated from the magnetic-lens chamber with a  $150 \mu\text{m}$  aluminum aperture which, in turn, is separated from the  $\text{LaB}_6$  cathode chamber by a 1 mm aperture. The resulting vacuum level of the cathode chamber is approximately  $10^{-7}$  mbar. The lens and cathode chambers are pumped by 56 and 60  $\ell/\text{s}$  turbo pumps, respectively.

The emitted x-ray radiation is characterized spectrally and spatially. For quantitative but broadband spectral measurements we employ a soft x-ray silicon drift detector (SDD) (Ref. 12) with  $\sim 70$  eV bandwidth (BW).<sup>13</sup> The SDD is placed 1.25 m from the source at right angles to the e-beam and water jet directions. A  $400 \mu\text{m}$  diameter aperture limits the incoming photon flux to ensure error-free single-photon counting. For high-resolution relative spectral measurement, the aperture/SDD arrangement is exchanged for a 10 000 lp/mm transmission grating/soft x-ray charge coupled device (CCD) detector arrangement.<sup>14</sup> The source-grating and source-detector distances are 0.9 and 1.8 m, respectively, resulting in an estimated resolution of  $\lambda/\Delta\lambda = 180$  (2.9 eV at 525 eV) assuming a  $12 \mu\text{m}$  spot (cf. below). Finally, the x-ray source size was measured by imaging the spot with an in-house fabricated Ni zone-plate (ZP) onto the CCD. This  $500 \mu\text{m}$  diameter ZP has 240 zones and an outer zone width of 477 nm resulting in a 93 mm focal length at 525 eV. A  $200 \mu\text{m}$  diameter tungsten wire is used as a central stop to block the background from high energy

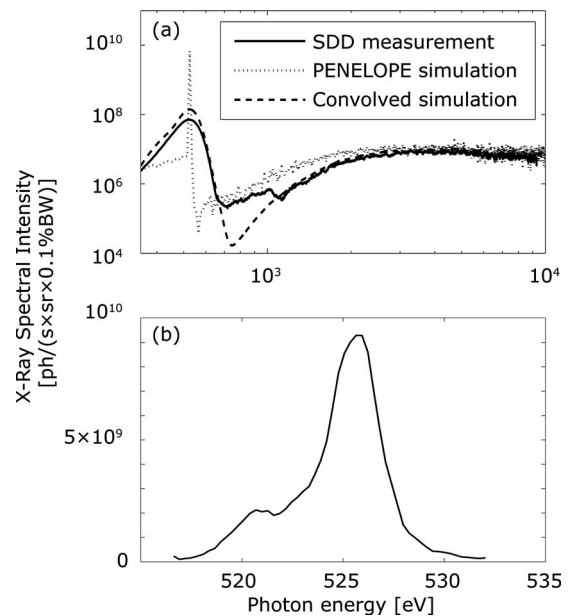


FIG. 2. (a) Experimentally recorded quantitative SDD spectrum of the electron-impact water-jet x-ray emission (solid line). Dotted and dashed lines represent the PENELOPE simulated spectrum before and after detector-bandwidth convolution and absorption correction, respectively. (b) High-resolution spectrum of oxygen  $K_{\alpha}$  lines, calibrated by the SDD/PENELOPE data.

bremsstrahlung. With a source-detector distance of 1.8 m the magnification is  $17\times$  and the Rayleigh resolution limit is  $0.6 \mu\text{m}$ . The exposure time was one second.

Figure 2(a) shows the measured x-ray spectral intensity recorded at 1.5 W e-beam power with the calibrated silicon drift detector (solid line). The BW of the detector clearly smooths the oxygen  $K_{\alpha}$  525 eV line emission while the  $>1$  keV broadband bremsstrahlung emission is less affected. In order to determine the quantitative 525 eV line emission we combine the SDD measurement with a PENELOPE simulation (10 eV bins, dotted line). The simulation is compensated for window absorption and convolved with a Gaussian function, and a 78 eV FWHM provides the best fit with the overall experimental data (dashed line). 78 eV agrees well with the approximate BW given by the manufacturer.<sup>13</sup> The convolved simulations and the experiments agree well, differing 35% in the 500 eV range. The resulting emission from the full 525 eV line is determined to  $7.5 \times 10^{10}$  ph/(s  $\times$  sr).

Figure 2(b) shows the high-resolution spectrum recorded with the 2.9 eV BW grating spectrometer at 2 W e-beam power. The spectral line is primarily due to the three molecular transitions at 526.8, 524.8, and 520.4 eV, but has been shown to be influenced by the local electronic structure due to hydrogen-bond formation by neighboring water molecules.<sup>15,16</sup> The measured bandwidth of the major unresolved 526.8/524.8 eV line is 3 eV, consistent with the spectrometer resolution. The spectrum is absolutely calibrated from the above procedure, conservatively assuming the experimentally determined bandwidth.

Figure 3 shows the total emitted soft x-ray intensity around the 525 eV line for e-beam powers between 1.5 and 7.8 W, ranging from  $7.5 \times 10^{10}$  to  $4.8 \times 10^{11}$  ph/(s  $\times$  sr  $\times$  line). It is clear that the intensity scales linearly with e-beam power. The measurement errors are primarily due to

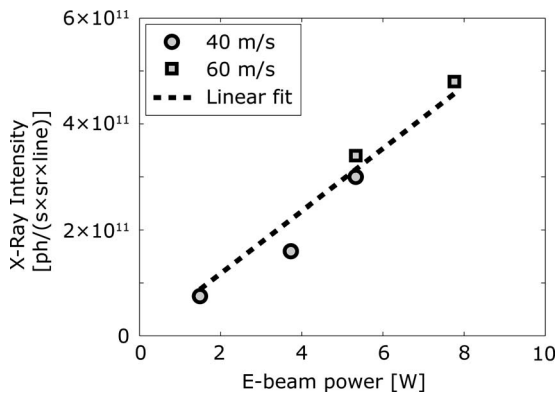


FIG. 3. Soft x-ray intensity at  $\sim 525$  eV as a function of electron-beam power. The dashed curve represents the linear fit.

a  $\pm 2\text{--}3$   $\mu\text{m}$  alignment uncertainty between the e-beam focus and the jet, which results in a  $\pm 20\%$ – $25\%$  variation in the x-ray intensity, primarily due to self absorption. Further increase in e-beam power is inadvisable in the present arrangement due to the rising pressure at the cathode.

Finally, the source size is measured with a zone-plate arrangement. This is necessary in order to determine the source brightness. Figure 1(b) shows the resulting  $19 \times 12$   $\mu\text{m}$  (FWHM) intensity distribution. The asymmetry is due to that most electrons are absorbed in the first part of the jet. Combining the measurements above we conclude that the average source brightness is  $3.0 \times 10^9$   $\text{ph}/(\text{s} \times \mu\text{m}^2 \times \text{sr} \times \text{line})$  at 7.8 W e-beam power. This corresponds to  $3.8 \times 10^8$   $\text{ph}/(\text{s} \times \mu\text{m}^2 \times \text{sr} \times \text{line} \times \text{W})$ . The source spatial stability, which is important for microscopy, is primarily influenced by high-frequency jet vibrations and slow thermal drifts. The high-frequency components are already included in the 1 s source-size measurements and the slow drifts are estimated to be less than a few  $\mu\text{m}$  for the present 15 min experiments.

Present state-of-the-art laser-plasma liquid-jet sources typically provide  $2\text{--}4 \times 10^{10}$   $\text{ph}/(\text{s} \times \mu\text{m}^2 \times \text{sr} \times \text{line})$  at the  $\lambda = 2.48$  nm (500 eV) line of nitrogen when operated at 100 Hz laser repetition rate.<sup>3</sup> Given the  $3.8 \times 10^8$   $\text{ph}/(\text{s} \times \mu\text{m}^2 \times \text{sr} \times \text{line} \times \text{W})$  above, the present source would achieve a similar brightness with 50–100 W of e-beam power, assuming brightness scales linearly with e-beam power. However, considering the need for narrow-band illumination in x-ray microscopy,<sup>6</sup> one must compensate for the larger line width of the present source. In short, we expect the new source to match the present state-of-the-art laser-plasma sources when operated at approximately 200 W, a factor 25 higher than demonstrated here.

PENELOPE simulations assumes that the x-ray emission is linear and scalable with power. However, this assumption requires that the target density and composition is constant. Fluid mechanical issues such as instabilities, boiling and evaporation, are not taken into account. Therefore the jet stability was investigated for e-beam powers between 1.5 and 7.8 W. Figure 1(c) shows images of the jet, recorded with an optical microscope mounted at a right angle to the e-beam and water jet directions. The images clearly illustrate the importance of jet speed for a stable jet target operation. In the left panel the jet is operated at low speed ( $v$

$= 40$  m/s) and the deterioration of the jet is evident as the power is increased from 1.5 to 5.3 W. The right panel shows  $v = 60$  m/s operation. Here 7.8 W is allowed without significant spray.

Stable operation of the jet under high-power e-beam loading is essential for scaling the power. Our experiments show that increasing the jet speed increases the stability. Furthermore, we have previously shown that a stable water jet can be operated at very high Reynold's numbers ( $5.4 \times 10^4$ ),<sup>17</sup> making a 2100 m/s 20  $\mu\text{m}$  jet feasible. Assuming that the instabilities grow linearly with e-beam power, this would make stable operation at  $> 250$  W of power possible. Furthermore, such a 2100 m/s, 20  $\mu\text{m}$  water jet system would be heated to approximately 70 °C by a 200 W, 30 kV e-beam, thereby remaining close to liquid-state density. We note that the heating is very rapid, the transit time is only 5 ns through a 10  $\mu\text{m}$  e-beam spot, which probably will result in spraylike instabilities down-stream. Unfortunately increased power loading results in increased background pressure which will affect the life time of the LaB<sub>6</sub> cathode. This can be handled with triple differentially pumped system. In summary, we feel confident that the present system can be stably operated at high power for x-ray microscopy as well as other soft x-ray applications such as photo-electron spectroscopy.

The authors thank Oscar Hemberg and co-workers at Excillum AB and Per Takman for valuable discussions, and Magnus Lindblom for fabricating the zone plate. The financial support of the Swedish Science Research Council and the Göran Gustafsson Foundation is gratefully acknowledged.

- <sup>1</sup>J. Kirz, C. Jacobsen, and M. Howells, *Q. Rev. Biophys.* **28**, 33 (1995); Proceedings of the International Conference on X-Ray Microscopy, 2008, edited by C. Quitmann, C. David, F. Nolting, F. Pfeiffer, and M. Stampfli [J. Phys.: Conf. Ser. 186 (2009)].
- <sup>2</sup>See, e.g., D. Attwood, *Soft X-rays and Extreme Ultraviolet Radiation* (Cambridge University Press, Cambridge, 2000).
- <sup>3</sup>P. A. C. Jansson, U. Vogt, and H. M. Hertz, *Rev. Sci. Instrum.* **76**, 043503 (2005).
- <sup>4</sup>M. Benk, K. Bergmann, D. Schäfer, and T. Wilhein, *Opt. Lett.* **33**, 2359 (2008).
- <sup>5</sup>L. Rymell and H. M. Hertz, *Opt. Commun.* **103**, 105 (1993).
- <sup>6</sup>M. Berglund, L. Rymell, M. Peucker, T. Wilhein, and H. M. Hertz, *J. Microsc.* **197**, 268 (2000).
- <sup>7</sup>O. Hemberg, M. Otendal, and H. M. Hertz, *Appl. Phys. Lett.* **83**, 1483 (2003).
- <sup>8</sup>M. Otendal, T. Tuohimaa, U. Vogt, and H. M. Hertz, *Rev. Sci. Instrum.* **79**, 016102 (2008).
- <sup>9</sup>T. Tuohimaa, J. Ewald, M. Schlie, H. M. Hertz, and U. Vogt, *Appl. Phys. Lett.* **92**, 233509 (2008).
- <sup>10</sup>B. Buijse, *Proc. SPIE* **4502**, 74 (2001).
- <sup>11</sup>X. Llovet, J. M. Fernández-Varea, J. Sempau, and F. Salvat, *Surf. Interface Anal.* **37**, 1054 (2005).
- <sup>12</sup>AXAS-D, [www.ketek.net/products/axas-systems/axas-d.html](http://www.ketek.net/products/axas-systems/axas-d.html).
- <sup>13</sup>S. Pahlke, KETEK GmbH, personal communication.
- <sup>14</sup>T. Wilhein, S. Rehbein, D. Hambach, M. Berglund, L. Rymell, and H. M. Hertz, *Rev. Sci. Instrum.* **70**, 1694 (1999).
- <sup>15</sup>J. Nordgren, L. O. Werme, H. Ågren, C. Nordling, and K. Siegbahn, *J. Phys. B* **8**, L18 (1975).
- <sup>16</sup>J. H. Guo, Y. Luo, A. Augustsson, J. E. Rubensson, C. Sâthe, H. A. Ågren, H. Siegbahn, and J. Nordgren, *Phys. Rev. Lett.* **89**, 137402 (2002).
- <sup>17</sup>M. Otendal, O. Hemberg, T. Tuohimaa, and H. M. Hertz, *Exp. Fluids* **39**, 799 (2005).